

Theory of vortex crystal formation in two-dimensional turbulence*

Dezhe Z. Jin[†] and Daniel H. E. Dubin

Physics Department, University of California at San Diego, La Jolla, California 92093

(Received 15 November 1999; accepted 28 December 1999)

Experiments on pure electron plasmas have found that the decay of two-dimensional (2D) turbulence can lead to spontaneous formation of “vortex crystals,” which are symmetric arrays of strong vortices within a background of weaker vorticity. This paper presents a theory of these novel equilibrium states of 2D turbulence. The paper consists of two parts. In the first part, we show that the vortex crystals are well described as “regional” maximum fluid entropy (RMFE) states, which are equilibrium states reached through ergodic mixing of the background by the strong vortices. In the second part, a theory is advanced that allows us to predict from the initial conditions the approximate number of the strong vortices in the final state. © 2000 American Institute of Physics. [S1070-664X(00)90705-5]

I. INTRODUCTION

Some properties of certain natural turbulent flows can be described by two-dimensional (2D) models. Examples of such flows include hurricanes, large scale ocean eddies, and the Great Red Spot on Jupiter.¹ The simplest model of freely relaxing 2D turbulence is the 2D Euler equation, in which the flow is inviscid and incompressible. In this model, the vorticity of the flow, $\omega(\mathbf{r}, t) = \nabla \times \mathbf{v}(\mathbf{r}, t)$, is convected by the velocity field $\mathbf{v}(\mathbf{r}, t)$ according to the Euler equation $\partial_t \omega + \mathbf{v} \cdot \nabla \omega = 0$. The stream function $\psi(\mathbf{r}, t)$ determines the velocity by $\mathbf{v} = \nabla \times \psi \hat{\mathbf{z}} = (\partial_y \psi, -\partial_x \psi)$, and is related to the vorticity via the Poisson's equation

$$\nabla^2 \psi = -\omega. \quad (1)$$

In this paper, we present a theory of “vortex crystals,” which are surprisingly complex yet ordered equilibria resulting from the inviscid relaxation of 2D turbulence. Vortex crystals were discovered in recent experiments by Fine *et al.*² The experiments were performed with pure electron columns, whose dynamics is isomorphic to the 2D Euler equation with free-slip boundary condition in a circular region (i.e., $\psi = 0$ on the circular boundary).² In the experiments, initial conditions are chosen so that strong vortices (compact patches of high vorticity) form due to a Kelvin–Helmholtz instability. The strong vortices move chaotically due to mutual advection, resulting in pairwise merger events and the formation of filamentary structures. These filaments are mixed by the flow, forming a low vorticity background. This turbulent flow then relaxes spontaneously to a vortex crystal equilibrium, in which a number of strong vortices remain and form a stable pattern in the low vorticity background. The equilibrium pattern of strong vortices persists for 10^4 turnover times of the column, until nonideal dissipation effects destroy the individual strong vortices. Several experimental images of the vortex crystals are displayed in the top row of Fig. 1.

Vortex crystals are not predicted by previous theories of freely decaying 2D turbulence. The inverse cascade theory of Batchelor proposes that the energy of 2D turbulence cascades to large scales.³ As a result, 2D turbulent flows are expected to decay into structures that have a typical dimension comparable to the system size. The statistical theory of 2D turbulence, initiated by Onsager⁴ and further developed by Joyce and Montgomery,⁵ Miller,⁶ and Robert and Sommeria,⁷ assumes that vorticity of a 2D turbulent flow is ergodically mixed. We refer to this theory as global maximum fluid entropy (GMFE) theory. Like Batchelor's theory, GMFE theory predicts smooth vorticity distribution over scales of system size in the relaxed states of turbulent flows. The existence of strong vortices with radius much smaller than the system size indicates that vortex crystals cannot be explained by either the inverse cascade theory or the statistical theory.

The emergence of isolated strong vortices in 2D turbulence has been previously observed in computer simulations.^{8,9} Based on these observations, Carnevale *et al.* proposed a punctuated scaling theory (PST).¹⁰ This theory describes 2D turbulence as a collection of strong vortices whose chaotic dynamics can be described by the Hamiltonian dynamics of point vortices punctuated by occasional mergers of like-sign strong vortices. The theory predicts that the number of strong vortices should decrease according to a power law, until only a single vortex (or a pair of opposite signed vortices) remains. The early evolution of the flows that form vortex crystals agrees with PST.² However, the theory does not explain why several strong vortices remain and form equilibrium patterns in the relaxed states.

In this paper, we show that vortex crystals form due to an interaction between the strong vortices and the low vorticity background. The key idea is to recognize that some regions of the flow are well-mixed, while other regions are not. The strong vortices ergodically mix the background, driving it toward a state of maximum fluid entropy. This mixing, in return, affects the punctuated dynamics of the strong vortices, “cooling” their chaotic motions, and driving them toward an equilibrium pattern. However, the vorticity in the strong vortices is trapped and remains unmixed. The

*Paper UI2 4 Bull. Am. Phys. Soc. **44**, 290 (1999).

[†]Invited speaker.

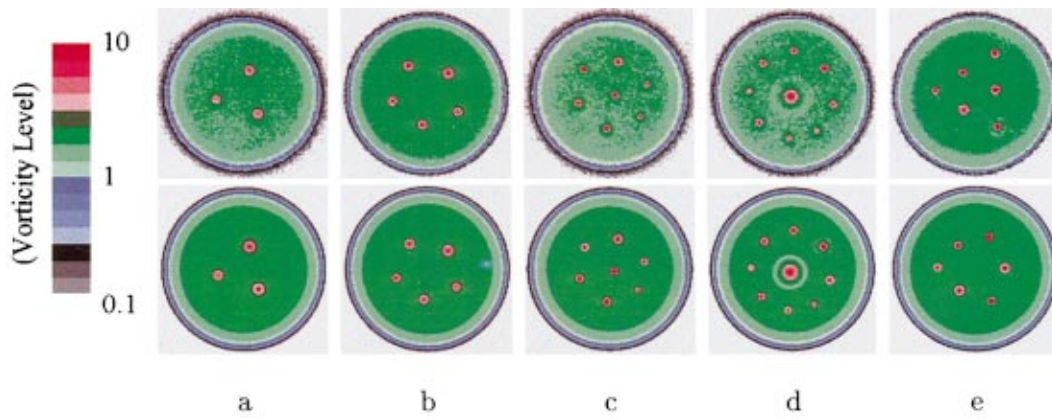


FIG. 1. (Color) Top: examples of experimental images of vortex crystal states (taken from Ref. 3). Bottom: corresponding regional maximum fluid entropy states. False color contour plots of vorticity are displayed.

resulting equilibrium is called a “regional” maximum fluid entropy (RMFE) state, in order to distinguish it from the GMFE state that allows no unmixed regions and hence no strong vortices. The RMFE theory predicts the positions of the strong vortices as well as the vorticity distribution of the background, provided that several conserved quantities of the 2D Euler flow are known; these include: the total circulation, total angular momentum, and total energy, as well as the number of strong vortices and the vorticity distributions in each strong vortex.

However, the RMFE theory must assume a given number of strong vortices remains in the final state. The second half of this paper outlines a method for predicting the number of strong vortices in the vortex crystal from characteristics of the initial flow. Two time scales are important: the average time τ_m between mergers, and the time τ_c required to cool the chaotic motions of the strong vortices through their interaction with the background. When τ_m becomes longer than τ_c , the strong vortices cool into a crystal state before the next merger event can occur and the mergers cease, leaving N_c vortices in the final state. Through estimation of τ_m and τ_c , we find that N_c can be predicted from the characteristics of the turbulent flows in the early stage of the relaxation.

II. RMFE THEORY

In this section, we show that vortex crystals can be explained by ergodic mixing of the background by the strong vortices. To do so, we first characterize the RMFE states, and then show that the vortex crystal states are well-described by RMFE states. More detailed presentations of the theory can be found in Refs. 11 and 12.

Ergodic mixing of the background, due mainly to the strong vortices, causes the background to approach a maximum fluid entropy state. To be more precise, the macroscopic state of the background, specified by a coarse-grained vorticity distribution $\omega_b(\mathbf{r})$, approaches a functional form that allows the maximum number of arrangements of the microscopic vorticity elements in the background. Since only vorticity elements in the background are mixed, this state is termed an RMFE state, to distinguish from the GMFE state that allows no unmixed regions.

The fluid entropy $S[\omega_b(\mathbf{r})]$ of the background can be calculated by counting the number of ways of arranging microscopic vorticity elements to obtain the given coarse-grained vorticity $\omega_b(\mathbf{r})$. For the simplest case of vorticity elements all having the same positive vorticity ω_f , the entropy is $S[\omega_b(\mathbf{r})] = -\int d\mathbf{r}^2 [p(\mathbf{r}) \ln p(\mathbf{r}) + (1-p(\mathbf{r})) \times \ln(1-p(\mathbf{r}))]$, where $p(\mathbf{r}) \equiv \omega_b(\mathbf{r})/\omega_f$.^{6,7} The second term is due to the incompressibility of the vorticity elements, and does not appear in the usual (Boltzmann) expression of the entropy for a point vortex flow.

Maximization of $S[\omega_b(\mathbf{r})]$ enables us to find the RMFE state. However, the maximization must be constrained by several dynamically conserved quantities. First, the flow conserves the total circulation $\Gamma = \int d\mathbf{r}^2 \omega$; the angular momentum $L = -\int d\mathbf{r}^2 \omega r^2/2$ (conserved since the flow is bounded by a free-slip circular boundary); and the energy $H = \int d\mathbf{r}^2 |\mathbf{v}|^2/2 = \int d\mathbf{r}^2 \psi \omega/2$. Second, the vorticity levels of the microscopic vorticity elements making up the background must be specified. Finally, the number N_c of the surviving strong vortices and the vorticity distributions $\zeta_i(|\mathbf{r} - \mathbf{R}_i|)$, $i = 1, \dots, N_c$ in each strong vortex are conserved. Here \mathbf{R}_i is the position of the i th strong vortex. (These properties of the strong vortices are dynamically conserved since we focus here on the evolution of the flow after mergers of the strong vortices have ceased.)

The maximization of S while keeping H , L , and Γ constant is carried out by finding the extrema of $S' \equiv S - \beta(H - \Omega L + \mu \Gamma)$ with respect to the independent variables $\{\mathbf{R}_i\}$ and $\omega_b(\mathbf{r})$. Here, β , Ω , and μ are Lagrange multipliers that can be interpreted as inverse temperature, rotation frequency, and the chemical potential, respectively. The extrema of S' with respect to $\{\mathbf{R}_i\}$ are given by

$$\frac{\partial S'}{\partial \mathbf{R}_i} = \frac{\partial}{\partial \mathbf{R}_i} (H - \Omega L) = 0. \quad (2)$$

Since $H - \Omega L$ is the Hamiltonian of the system in a frame rotating at frequency Ω , Eq. (2) shows that in the RMFE state the velocities of the strong vortices are zero in this rotating frame: in other words, the strong vortices are in equilibrium, rotating rigidly at frequency Ω .

The extremum of S' with respect to $\omega_b(\mathbf{r})$ is given by $\delta S' = 0$, i.e., $\int d\mathbf{r}^2 [\ln p(\mathbf{r}) - \ln(1-p(\mathbf{r})) + \beta \omega_f \phi] \delta \omega_b(\mathbf{r}) = 0$

for small, arbitrary $\delta\omega_b(\mathbf{r})$, where $\phi \equiv \psi + \frac{1}{2}\Omega r^2 + \mu$ is the stream function in the rotating frame. Therefore, the equilibrium vorticity distribution is predicted to be

$$\omega_b(\mathbf{r}) = \omega_f / (e^{\beta\omega_f\phi} + 1). \quad (3)$$

This is very similar to the Fermi distribution in quantum statistics, which is not unexpected since the microscopic vorticity elements are incompressible.

We now show that the observed vortex crystals are well-described by RMFE states. From an experimental flow, we first determine the number of the strong vortices N_c by counting the clumps with local vorticity extrema much larger than the average vorticity of the flow. Next, the vorticity distribution in the i th strong vortex ($i = 1, \dots, N_c$) is specified by the vorticity radial profile $\zeta_i(|\mathbf{r} - \mathbf{R}_i|)$ around the local extremum. The vorticity profile (rather than merely the circulation) of each strong vortex is required because the self-energy of the strong vortex must be included in H .

In order to completely specify the problem, we must choose a value for the Fermi vorticity ω_f associated with the vorticity elements of the background. In fact, the general theory allows for a distribution of values for ω_f ,^{6,7} but we have found that a single value is sufficient to explain the experiments: $\omega_f = 2.15$ is used in all of our calculations. A discussion of the physical reasoning behind this choice can be found in Refs. 11 and 12. Lengths are scaled by r_w (the radius of the circular free-slip boundary), and vorticities are scaled by Γ/r_w^2 .

Along with ω_f and ζ_i , we also evaluate the conserved quantities H , L , and Γ from the experimental flow using their previous definitions. These inputs from the experimental flow determine the corresponding RMFE state with no free parameters. For fixed ω_f and ζ_i we numerically search for the proper values of β , Ω , and μ needed to match the experimental values of H , L , and Γ , with the background vorticity given by Eq. (3). Meanwhile, we also search for $\{\mathbf{R}_i\}$, $i = 1, \dots, N_c$, so that Eq. (2) is satisfied.

The RMFE solutions reproduce the observed vortex crystal patterns and the observed background vorticity, as shown in Fig. 1.

III. ESTIMATION OF N_c

In the previous section, the number N_c of strong vortices in the vortex crystal was not predicted by the theory; rather, it was merely taken as an experimental input. In this section we show that N_c can be roughly estimated from certain characteristics of the turbulent flow in the early stages.

The analysis depends on the physical picture of vortex crystal formation discussed in the Introduction. In particular, we need to estimate the average time between successive merger events, τ_m , and the ‘‘cooling’’ time τ_c , defined as the time scale for the vortices to cool into a vortex crystal.

We can estimate τ_m from the observed time evolution $N(t)$ of the number of the strong vortices in the early stage of the turbulent evolution. As previously discussed in connection with PST, numerical simulations⁸ and experiments^{2,14} have found that $N(t)$ evolves according to a power law

$$N(t) = N(t_0)(t/t_0)^{-\xi}, \quad (4)$$

where $\xi > 0$ is a constant, and t_0 is any time chosen from the range of times where the power law scaling is observed. (Typically, this time range does not include the initial condition of the flow, since it often takes some time for the strong vortices to form.) Other quantities associated with the strong vortices also evolve in time according to power laws. For example, the average circulation per vortex of the strong vortices, $\bar{\Gamma}(t)$, increases in time as

$$\bar{\Gamma}(t) = \bar{\Gamma}(t_0)(t/t_0)^{\eta\xi}, \quad (5)$$

where $\eta > 0$ is a constant. Although PST predicts fixed values for the exponents, we find that their values vary in different experiments and simulations. We therefore take Eqs. (4) and (5) as empirical laws, and measure η and ξ separately from each flow.

The average time τ_m between successive mergers is given by the time required for the number of the strong vortices to decrease by 1: $\Delta N = -1$. For large N , $\Delta N/\tau_m = -1/\tau_m \approx dN/dt = -\xi N(t_0)(t/t_0)^{-1-\xi}/t_0$, where in the last step Eq. (4) was used. Therefore,

$$\tau_m \approx -1/(dN/dt) = t_0 \xi^{-1} N(t_0)^{-1} (t/t_0)^{1+\xi}. \quad (6)$$

The cooling time scale τ_c is estimated from the time scale for the strong vortices to completely randomize the background flow. This is the time scale for vorticity elements of the background to be distributed randomly, and hence the time scale for the background to approach to the maximum entropy state, in which the strong vortices are in equilibrium.

Assuming that the strong vortices are primary mixers of the background, we can estimate the complete randomization time of the background by treating the strong vortices as point vortices, and the background as passive scalars. We then study the chaotic advection of passive scalars in the fields of point vortices in order to understand the mixing of the background. This approach to understanding complex fluid mixing was pioneered by Aref.^{15,16}

The trajectory of a passive scalar is chaotic if its Lyapunov exponent λ is positive, nonchaotic otherwise. The Lyapunov exponent of a trajectory is defined in terms of the difference $\delta\mathbf{r}(t) = \mathbf{r}_1(t) - \mathbf{r}_2(t)$ of two infinitesimally close trajectories, $\mathbf{r}_1(t)$ and $\mathbf{r}_2(t)$: $\lambda = \lim_{t \rightarrow \infty} t^{-1} \ln(|\delta\mathbf{r}(t)|/|\delta\mathbf{r}(0)|)$. Since the rate of mixing of the passive scalars in the flow field of the point vortices is given by the Lyapunov exponents λ of the chaotic trajectories of the passive scalars, we identify the inverse cooling time τ_c^{-1} with the average Lyapunov exponent $\bar{\lambda}$ of a collection of passive scalars, counting only those passive scalars with positive λ .

We can estimate $\bar{\lambda}$ with dimensional analysis. When the point vortices have approximately equal circulations and their motions are chaotic in a region of area A , the main physical quantities that determine $\bar{\lambda}$ are the average circulation $\bar{\Gamma}$ of the point vortices and the average distance $D = \sqrt{A/N}$ between the nearby point vortices. This implies that

$$\tau_c^{-1} = \bar{\lambda} \approx \alpha \bar{\Gamma}/D^2 = \alpha \Gamma_T/A, \quad (7)$$

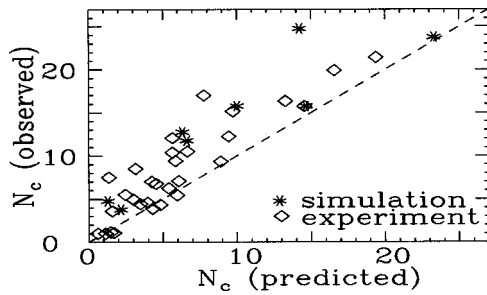


FIG. 2. Comparison of the predicted number N_c of the strong vortices in the vortex crystals with the N_c of the experiments and the simulations. Each data point represents a particular evolution of the turbulent flow.

where α is a constant, and $\Gamma_T = N\bar{\Gamma}$ is the total circulation of the point vortices. Numerical calculations confirm Eq. (7), with $\alpha \approx 0.031$.^{12,13}

The cooling time τ_c depends on the total circulation of the strong vortices, which decreases as the strong vortices merge. From Eqs. (4) and (5), we obtain $\Gamma_T(t) = N(t_0)\Gamma(t_0)(t/t_0)^{\eta\xi - \xi}$. Therefore, from Eq. (7) we find that the cooling time increases as the flow evolves

$$\tau_c \approx \frac{A}{\alpha N(t_0)\bar{\Gamma}(t_0)} \left(\frac{t}{t_0} \right)^{\xi - \eta\xi}. \quad (8)$$

Comparison of Eqs. (6) and (8) shows that τ_c grows in time more slowly than τ_m since $\eta > 0$. Therefore, starting from $\tau_m < \tau_c$, τ_m will eventually catch up with τ_c at $t = t_1$, and mergers of the strong vortices will stop. Here, t_1 is found by setting $\tau_c \approx \tau_m$, and from Eqs. (6) and (8) we arrive at $t_1 \approx t_0 (\xi A / \alpha t_0 \bar{\Gamma}(t_0))^{1/(1+\eta\xi)}$. Accordingly, the number of the strong vortices in the vortex crystals is obtained by setting $t = t_1$ in Eq. (4)

$$N_c \approx N(t_0) \left(\frac{\alpha t_0 \bar{\Gamma}(t_0)}{\xi A} \right)^{\xi/(1+\eta\xi)}. \quad (9)$$

This equation shows that in order to form vortex crystals with many surviving strong vortices, initially the flow should have a large number of strong vortices with large average circulation, concentrated in a small area.

In Fig. 2, we plot the predicted N_c from Eq. (9), averaged over the power law region of $N(t)$, against the observed N_c for the experiments and simulations. In the experiment the observed N_c fluctuates because of shot noise.² Therefore, we take the average value of the observed N_c .

Figure 2 shows that the prediction of Eq. (9) clearly distinguishes the characteristics of flows that form vortex crystals with many strong vortices from those of flows that form no vortex crystals. However, the scatter in the data is quite large. This might be expected, given that the process of vortex crystal formation is chaotic. The observed N_c tends to be larger than that predicted from Eq. (9). It appears that the strong vortices are relaxing to equilibrium more rapidly than our estimation for τ_c would predict. The exact reason why

this is so is not completely understood. One possibility is that our model assumes that the strong vortices are randomly distributed after each merger event, requiring a full cooling time τ_c to relax to equilibrium. However, by the time of last merger event, the strong vortices are no longer randomly distributed, and may be close to their equilibrium positions.

IV. DISCUSSION

Until now, vortex crystals have only been observed in turbulent flows with a single sign of vorticity, subject to a circular, free-slip boundary condition. It is of interest to determine whether vortex crystals can form in more general cases with both signs of vorticity and/or different boundary conditions. As we have shown in this paper, one requirement is that there should be many strong vortices in the initial stages of the turbulent flow. Our theory also suggests that two conditions are crucial for vortex crystal formation. First, calculations similar to those we have done in Ref. 11 should be carried out for more general flows to reveal that ordered, stable structures for the strong vortices can emerge by maximization of the fluid entropy of the low vorticity background. The second condition is that the mixing time scale τ_c of the background must be sufficiently fast. This can be investigated by considering the chaotic advection of point vortices, as we have done in Ref. 13. It is conceivable that τ_c can vary considerably depending on the characteristics of the turbulent flow. For example, if there are an approximately equal number of similar-sized positive and negative strong vortices, the mixing of the background may not be as efficient as the case we have studied in this paper, since the opposite signed strong vortices tend to form dipole pairs and hence at least partially cancel each other's mixing ability.

ACKNOWLEDGMENTS

We thank Professor T. M. O'Neil for invaluable suggestions, and thank Dr. K. S. Fine, Dr. A. C. Cass, and Professor F. C. Driscoll for providing the experimental data and useful discussions. This work was supported by National Science Foundation Grant No. PHY-9876999 and Office of Naval Research Grant No. N00014-96-1-0239.

¹D. G. Dritschel and B. Legras, *Phys. Today* **46**, 44 (1993).

²K. S. Fine, A. C. Cass, W. G. Flynn, and C. F. Driscoll, *Phys. Rev. Lett.* **75**, 3277 (1995).

³G. K. Batchelor, *Phys. Fluid. Supplement II*, II-233 (1969).

⁴L. Onsager, *Nuovo Cimento Suppl.* **6**, 279 (1949).

⁵G. Joyce and D. Montgomery, *J. Plasma Phys.* **10**, 107 (1973).

⁶J. Miller, *Phys. Rev. Lett.* **65**, 2137 (1990).

⁷R. Robert and J. Sommeria, *J. Fluid Mech.* **229**, 291 (1991).

⁸J. C. McWilliams, *J. Fluid Mech.* **146**, 21 (1984).

⁹R. Benzi, S. Patarnello, and P. Santangelo, *Europhys. Lett.* **3**, 811 (1987).

¹⁰G. F. Carnevale, J. C. McWilliams, Y. Pomeau *et al.*, *Phys. Rev. Lett.* **66**, 2735 (1991).

¹¹D. Z. Jin and D. H. E. Dubin, *Phys. Rev. Lett.* **80**, 4434 (1998).

¹²D. Z. Jin, Ph.D. thesis, University of California, San Diego (1999).

¹³D. Z. Jin and D. H. E. Dubin, *Phys. Rev. Lett.* **84**, 1443 (2000).

¹⁴P. Tabeling, S. Burkhart, O. Cardoso *et al.*, *Phys. Rev. Lett.* **67**, 3772 (1991).

¹⁵H. Aref, *J. Fluid Mech.* **143**, 1 (1984).

¹⁶J. M. Ottino, *Annu. Rev. Fluid Mech.* **22**, 207 (1990).